IEEE Access
Multidisciplinary | Rapid Review | Open Access Journal

IEEE ENGINEERING IN MEDICINE AND BIOLOGY SOCIETY SECTION

Received January 9, 2020, accepted January 21, 2020, date of publication January 27, 2020, date of current version January 31, 2020.

Digital Object Identifier 10.1109/ACCESS.2020.2969720

LSTM Improves Accuracy of Reaching Trajectory Prediction From Magnetoencephalography Signals

HONG GI YEOM[1], JUNE SIC KIM[2], AND CHUN KEE CHUNG[2,3,4]

[1]Department of Electronics Engineering, Chosun University, Gwangju 61452, South Korea
[2]Department of Brain and Cognitive Sciences, College of Natural Sciences, Seoul National University, Seoul 08826, South Korea
[3]Interdisciplinary Program in Neuroscience, Seoul National University, Seoul 08826, South Korea
[4]Department of Neurosurgery, Seoul National University College of Medicine and Hospital, Seoul 03080, South Korea

Corresponding author: June Sic Kim (jskim@hbf.re.kr)

This work was supported by the Research Fund from Chosun University, 2017.

ABSTRACT Brain-computer interface (BCI) is a promising and very helpful technology. BCI studies have attempted to predict arm movements to control robotic arm depending on movement intentions. However, the low accuracy of movement prediction is a critical challenge in predicting arm movements. The aim of this study was to predict arm movement with high accuracy from non-invasive neural signals using the deep learning algorithm. We compared the prediction accuracies of the conventional method and long short-term memory (LSTM) using non-invasive MEG signals. This is the first study that applied LSTM to predict arm movements from non-invasive neural signals. The coefficients of correlation between real signals and signals predicted by the MLR on the x-, y-, and z-axes were 0.677 ± 0.139 (mean $\pm$ SD), 0.689 ± 0.140, and 0.785 ± 0.103, respectively. The coefficients of correlation between real signals and signals predicted by the LSTM on the x-, y-, and z-axes were 0.978 ± 0.004, 0.980 ± 0.005, and 0.980 ± 0.008, respectively. The prediction accuracy was highly improved using the LSTM algorithm. Our results suggest that highly accurate prediction of arm movement is possible without surgery using the deep learning algorithm. We expect that the deep learning algorithm will facilitate the control of a robot arm using non-invasive signals in real life.

INDEX TERMS Brain-computer interface, deep learning, long short-term memory.

I. INTRODUCTION

The brain-computer interface (BCI) is a promising technology that can be used to predict user's intention and control electric devices without movements. It facilitates individuals with disability to express their thoughts or to control electric devices. Several types of BCI can be used to predict user's intentions [1]. First, the sensorimotor rhythm (SMR)-based BCI uses brain features suggesting that different areas of the brain have different functions [2]–[5]. For example, the left portion of the brain controls the right arm and the right half of the brain controls the left arm. Therefore, the spatial pattern of brain activity can be changed according to movement intention. The SMR-based BCI is generally used to select a direction according to movement intention, and can be used to control a mouse cursor or an electrical wheelchair.

The associate editor coordinating the review of this manuscript and approving it for publication was Emil Jovanov.

The second method is a P300-based BCI in which P300 represents a positive peak after exposure to a stimulus for about 300 ms [4], [6]. When a P300 BCI user is exposed to flashing characters, the magnitude of P300 increases during the focus on the stimulus. Therefore, the BCI user can select a character with a maximum amplitude of P300. The P300 BCI is usually utilized to type characters. The third type of BCI is steady-state visual-evoked potential (SSVEP). When exposed to blinking visual stimuli, the activity of the visual cortex peaks at the same frequency as the stimulus, and SSVEP BCI selects a visual target based on the characteristics. These types of BCI are useful to control a computer cursor or to select characters. However, they are limited in choice, and each selection requires repeated trials. Thus, the BCI users cannot select new choices except predetermined commands such as the directions or the characters.

To overcome the weakness, BCI researchers attempted to predict arm movements using neural signals to control

the robotic arm according to movement intentions [7]–[11]. It is an ideal method enabling users with any task intended. In this study, this type of BCI is designated as arm-movement prediction (AMP). In 1982, Georgopoulos discovered an important characteristic of neural activity in primary motor cortex (M1) [12]. The feature explains how specific neurons in the M1 prefer movement direction, suggesting that the firing rate of the neuron increases when it is closer to a specific direction. Reaching trajectory can be estimated from neural activities using the characteristic. Many studies have predicted arm movements from spike activity [13]–[15], local field potentials (LFPs) [16], [17], electrocorticography (ECoG) [18]–[21], EEG [22]–[25] and magnetoencephalography (MEG) [8], [9] in monkeys or humans. In 2008, the BCI study used monkeys to control a robotic arm in real time using neural activity [11]. In 2012, another research group reported that people with tetraplegia can drink coffee by controlling a robotic arm in real time via neural activity [7]. Although the task was successful, previous AMP BCI studies reported a low accuracy of prediction, which was even lower when the AMP BCI used non-invasive neural signals. The low accuracy of movement prediction is a critical challenge limiting the practical application of AMP BCI.

Recent machine learning studies showed that deep learning algorithm increase the prediction accuracy significantly. However, it has not been used in movement prediction using non-invasive neural signals. Therefore, this study investigated whether reaching trajectory could be predicted with high accuracy using deep learning from non-invasive neural signals. We compared the prediction accuracies of the conventional method with the deep learning algorithm.

II. MATERIALS AND METHODS

A. DATA ACQUISITION

To test the prediction accuracy, we used the same dataset as in our previous study that predicts arm movements from non-invasive MEG signals [8]. The same signal processing procedure was also used to extract features as described [8]. Briefly, nine right-handed healthy subjects including five males and four females (age, 19–37 years) participated in the study. A 306-channel whole-head MEG system (VectorView TM, Elekta Neuromag Oy, Helsinki, Finland) was used to measure the MEG signals during arm movements. Head movements were restricted by placing subjects' head in a fixed MEG helmet. Temporal Signal Space Separation (tSSS) filtering was performed to reduce external artifacts. Trajectories of arm movements were recorded using a three-axis accelerometer (KXM52, Kionix, NY, USA). The accelerometer was placed on the index finger and the sensor signals were simultaneously recorded with the MEG signals. To guide three-dimensional arm movements, stereographic images were presented on a screen. At the beginning of the experiment, a sphere was presented on the center of the screen. After 4 s, a target sphere with a stick connected to the center sphere appeared in one corner for 1 s. The target sphere was presented randomly in one of the four corners (upper-left, upper-right, bottom-left, and bottom-right). During this time, the subject was instructed to use his/her arm and to reach his/her index finger from the center to the target and return to the center along the stick line (center-out-center paradigm). For each subject, 60 trials were measured for each direction.

B. PREDICTION

To predict the movement, the signal processing was performed as follows [8].

The 68-channel MEG signals in motor-related areas were selected to reduce the effect of artifacts. After band-pass filtering at 0.5–8Hz, the MEG signals were downsampled to 50Hz. Eleven data points preceding the current data point were used to predict movement velocity. The velocities of arm movement on x, y, and z axes were predicted using multiple linear regression (MLR) and long short-term memory (LSTM). MLR is a general and popular method that shows a good prediction performance [7], [8], [22]–[24], [26]. LSTM is a state-of-the art deep-learning algorithm. We investigated whether the deep-learning algorithm improves prediction accuracy or not. All signal processing steps were performed using a MATLAB 2018a (Mathworks, Natick, MA, USA). The prediction techniques using MLR and LSTM are discussed below.

C. MULTIPLE LINEAR REGRESSION (MLR)

MLR is a linear algorithm to model the relationship between inputs and outputs sequentially. Eleven points of 68 channels (for a total of 748 points) were used as the features, and the x, y and z velocities of the movements were estimated using an MLR method, as follows:

$$x(t) = \sum_{i=1}^{n}\sum_{j=0}^{m} W_{ij}^{x} \times S_i(t-j) + W_0^{x}$$

$$y(t) = \sum_{i=1}^{n}\sum_{j=0}^{m} W_{ij}^{y} \times S_i(t-j) + W_0^{y}$$

$$z(t) = \sum_{i=1}^{n}\sum_{j=0}^{m} W_{ij}^{z} \times S_i(t-j) + W_0^{z}$$

where $x(t)$, $y(t)$ and $z(t)$ are the movement velocities estimated at time t. W_{ij}^{x}, W_{ij}^{y} and W_{ij}^{z} represent the weight value matrices obtained using the regression methods, and S_i is a MEG signal of channel i. The function n denotes the number of channels (68 in this study); m is the number of data points before time t, which determines the number of past data points that were used to estimate the current velocities $x(t)$, $y(t)$ and $z(t)$. The parameter j refers to time lag. W_0 is the constant used to compensate for errors. W_{ij} and W_0 were obtained by training using MLR.

D. LONG SHORT-TERM MEMORY (LSTM)

LSTM is a deep learning algorithm used to predict sequential data [27]–[29]. The key idea of LSTM is to remember

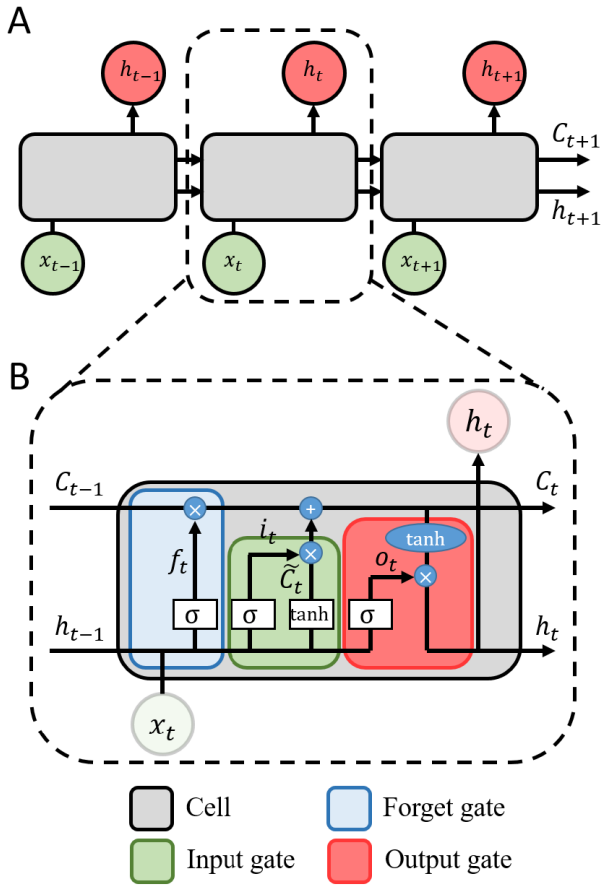

FIGURE 1. (A) A diagram of the LSTM. The green and red circles represent inputs and outputs, respectively. The gray squares indicate cells that process data. x_t is an input at time t; h_t is an output at time t; c_t is a cell state at time t. (B) A diagram of the cell. LSTM can retain the cell information over time. LSTM can delete or add information to the cell state using gates. There are three gates in one cell. The blue square is a 'forget' gate that determines the information indicated for deletion from the cell state. The green square represents an input gate that decides the information for addition to the cell state. The red square is an output gate that decides the output.

input information for long periods to predict outputs [27]. LSTM is usually composed of a cell and three gates, and can gradually retain the information through the cell. LSTM can delete or add information to the cell state via gates. Fig. 1 shows a diagram of the LSTM (modified from [21]). The 'forget' gate determines what information will be removed from the cell state. The input gate decides what information will be added to the cell state. The output gate decides the output. In Fig. 1, x_t is an input at time t; h_t is an output at time t; c_t is a cell state at time t. Gates determine the deletion or addition of information and output using following equations.

$$
\begin{aligned}
i_t &= \sigma\left(W_i \cdot [h_{t-1}, x_t] + b_i\right) \\
\tilde{C}_t &= tanh\left(W_C \cdot [h_{t-1}, x_t] + b_C\right) \\
C_t &= f_t * C_{t-1} + i_t * \tilde{C}_t \\
o_t &= \sigma\left(W_o \cdot [h_{t-1}, x_t] + b_o\right) \\
h_t &= o_t * \tanh(C_t)
\end{aligned}
$$

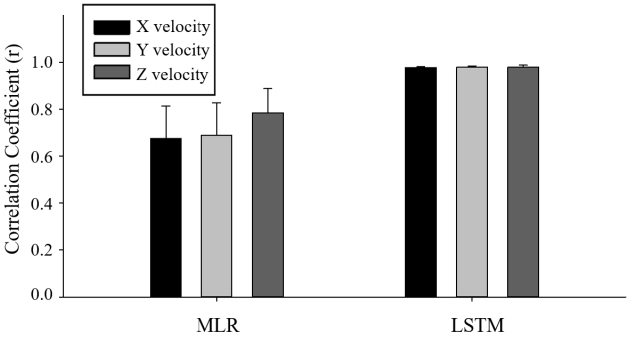

FIGURE 2. Averaged Pearson's correlation coefficients (r) between real and predicted movement trajectories with standard deviations for all subjects. The correlation coefficients between real signals and signals predicted by the MLR on the x-, y-, and z-axes were 0.677 ± 0.139, 0.689 ± 0.140, and 0.785 ± 0.103, respectively. The correlation coefficients between real signals and signals predicted by the LSTM along the three axes were 0.978 ± 0.004, 0.980 ± 0.005, and 0.980 ± 0.008, respectively.

Before training the LSTM algorithm, the MEG signals and movement trajectories were normalized by subtracting the mean and dividing with the standard deviation. The output size of the LSTM was 3 corresponding to the movement dimensions. The input size of the LSTM was 68, which is the channel number corresponding to the feature number. The number of hidden units was 200. The configurations of LSTM layers included a sequence input layer, an LSTM layer, a fully connected layer, a dropout layer, a fully connected layer and a regression layer. The maximum epoch number was 60. The size of mini batch was 20. The initial learning rate was 0.01. The gradient threshold was 1. These parameters were determined based on Matlab examples. The LSTM algorithm was trained with the training data comprising MEG signals and movement trajectories. After the training, the LSTM algorithm predicted the movement trajectories from test MEG data.

To implement deep learning, parameter determination is important. According to the number of hidden units, accuracy of the deep learning and learning time will be quite different. The number of hidden units were tested from 50 to 300.

E. EVALUATION OF THE PERFORMANCE

A five-fold cross-validation was used to assess the accuracy of decoding. This method separates the data into four-fifths for training and one-fifth for testing [30]. Thus, five combinations of training and testing data were available. Weights of the MLR and the LSTM were calculated from the training data, and the estimation accuracy was evaluated using the test data by calculating Pearson's correlation coefficients (r) between the real and estimated movement trajectories for each cross-validation fold. The correlation coefficients were averaged across the cross-validation folds and sessions.

III. RESULTS

The correlation coefficients between real signals and signals predicted by the MLR on the x-, y-, and z-axes were 0.677 ± 0.139 (mean ± SD), 0.689 ± 0.140, and 0.785 ± 0.103,

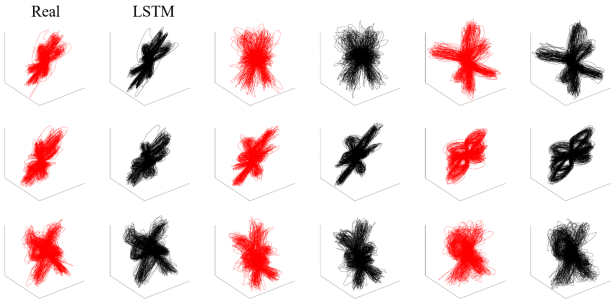

FIGURE 3. The results of prediction using LSTM in all subjects. The red lines show real movement trajectories. The black lines present the predicted movements. Each figure describes the result of a single subject.

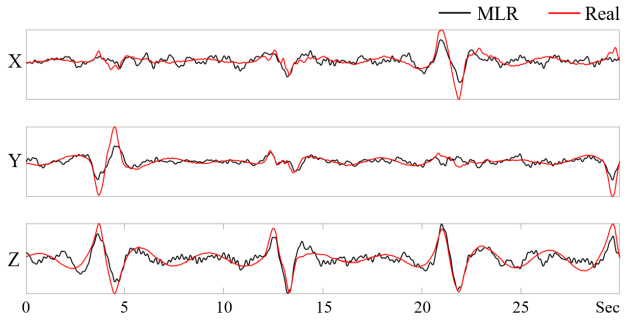

FIGURE 4. Sample results predicted by MLR. Each row shows a result on the x-, y-, and z-axes, respectively. The red lines show real movement trajectories. The black lines present the predicted movements.

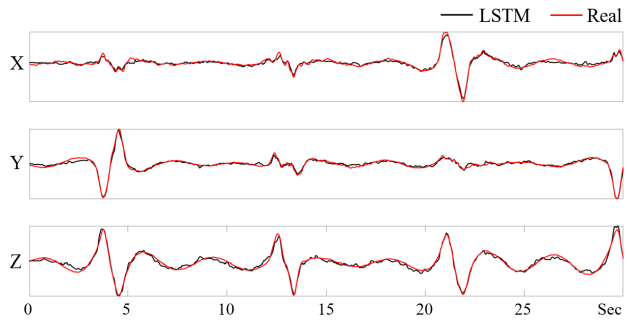

FIGURE 5. Sample results predicted by LSTM. Each row shows a result on the x-, y-, and z-axes, respectively. The red lines show real movement trajectories. The black lines present the predicted movements.

respectively. The correlation coefficients between real signals and signals predicted by the LSTM on the x-, y-, and z-axes were 0.978 $\pm$ 0.004, 0.980 $\pm$ 0.005, and 0.980 $\pm$ 0.008, respectively. The results are illustrated in Fig. 2. The prediction results of LSTM for all subjects are shown in Fig. 3. The red lines show real movement trajectories. The black lines present the predicted movements. Each figure describes the result of one subject. Fig. 4 and Fig. 5 depict sample results predicted by MLR and LSTM, respectively. The results of each row are displayed on the x-, y-, and z-axes. The red lines show real movement trajectories. The black lines present the predicted movements. Based on the results, it is clear that LSTM significantly improves the prediction accuracy. Moreover, the trajectories predicted by the LSTM are very similar to the real-movement trajectories.

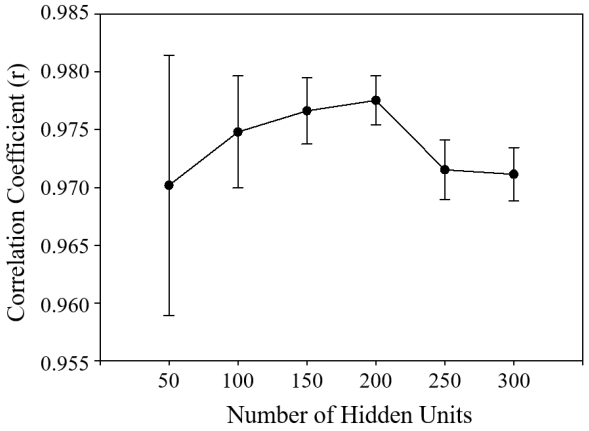

FIGURE 6. Averaged correlation coefficients between real and LSTM with standard deviations across all subjects, trials and axes according to the number of hidden units.

The correlation coefficient between real signals and signals predicted by the LSTM was maximum when the number of hidden units was 200 as shown in Fig. 6. The dots are averages of the correlation coefficients across all subjects, trials and axes. Error bars indicate the standard errors of the means.

IV. CONCLUSION

In this study, we compared the prediction accuracies of the conventional method MLR and the LSTM using non-invasive MEG signals. This is the first study that applied LSTM to predict arm movements using non-invasive neural signals. We showed that the prediction accuracy was significantly improved using the LSTM algorithm. The low accuracy of movement prediction was a critical limitation of the AMP BCI for real-world application. Our results indicate that highly accurate prediction of arm movement is possible without surgery using the deep learning algorithm. Based on our results, a robot arm can be controlled using non-invasive signals based on deep learning algorithms in real life.

REFERENCES

[1] G. Dornhege, *Toward Brain-Computer Interfacing* (Neural Information Processing). Cambridge, MA, USA: MIT Press, 2007, p. 507.

[2] E. R. Kandel, *Principles of Neural Science*, 5th ed. New York, NY, USA: McGraw-Hill, 2013, p. 1709.

[3] M.-C. Corsi, M. Chavez, D. Schwartz, L. Hugueville, A. N. Khambhati, D. S. Bassett, and F. De Vico Fallani, "Integrating EEG and MEG signals to improve motor imagery classification in brain–computer interface," *Int. J. Neur. Syst.*, vol. 29, no. 01, Feb. 2019, Art. no. 1850014, doi: 10.1142/s0129065718500144.

[4] F. Lotte, L. Bougrain, A. Cichocki, M. Clerc, M. Congedo, A. Rakotomamonjy, and F. Yger, "A review of classification algorithms for EEG-based brain–computer interfaces: A 10 year update," *J. Neural Eng.*, vol. 15, no. 3, Jun. 2018, Art. no. 031005, doi: 10.1088/1741-2552/aab2f2.

[5] S. Roy, D. Rathee, K. Mccreadie, and G. Prasad, "Channel selection improves MEG-based brain-computer interface," in *Proc. 9th Int. IEEE/EMBS Conf. Neural Eng. (NER)*, San Francisco, CA, USA, Mar. 2019, pp. 295–298.

[6] Z. Oralhan, "A new paradigm for region-based P300 speller in brain computer interface," *IEEE Access*, vol. 7, pp. 106618–106627, 2019, doi: 10.1109/access.2019.2933049.

[7] L. R. Hochberg, D. Bacher, B. Jarosiewicz, N. Y. Masse, J. D. Simeral, J. Vogel, S. Haddadin, J. Liu, S. S. Cash, P. Van Der Smagt, and J. P. Donoghue, "Reach and grasp by people with tetraplegia using a neurally controlled robotic arm," *Nature*, vol. 485, no. 7398, pp. 372–375, May 2012, doi: 10.1038/nature11076.
[8] H. G. Yeom, J. S. Kim, and C. K. Chung, "Estimation of the velocity and trajectory of three-dimensional reaching movements from non-invasive magnetoencephalography signals," *J. Neural Eng.*, vol. 10, no. 2, Apr. 2013, Art. no. 026006, doi: 10.1088/1741-2560/10/2/026006.
[9] H. G. Yeom, J. S. Kim, and C. K. Chung, "High-accuracy brain-machine interfaces using feedback information," *PLoS ONE*, vol. 9, no. 7, Jul. 2014, Art. no. e103539, doi: 10.1371/journal.pone.0103539.
[10] J. L. Collinger, B. Wodlinger, J. E. Downey, W. Wang, E. C. Tyler-Kabara, D. J. Weber, A. J. Mcmorland, M. Velliste, M. L. Boninger, and A. B. Schwartz, "High-performance neuroprosthetic control by an individual with tetraplegia," *Lancet*, vol. 381, no. 9866, pp. 557–564, Feb. 2013, doi: 10.1016/s0140-6736(12)61816-9.
[11] G. M. Mckhann, "Cortical control of a prosthetic arm for self-feeding," *Neurosurgery*, vol. 63, no. 2, pp. N8–N9, Aug. 2008, doi: 10.1227/01.neu.0000335797.80384.06.
[12] A. Georgopoulos, J. Kalaska, R. Caminiti, and J. Massey, "On the relations between the direction of two-dimensional arm movements and cell discharge in primate motor cortex," *J. Neurosci.*, vol. 2, no. 11, pp. 1527–1537, Nov. 1982.
[13] J. Wessberg, C. R. Stambaugh, J. D. Kralik, P. D. Beck, M. Laubach, J. K. Chapin, J. Kim, S. J. Biggs, M. A. Srinivasan, and M. A. L. Nicolelis, "Real-time prediction of hand trajectory by ensembles of cortical neurons in primates," *Nature*, vol. 408, no. 6810, pp. 361–365, Nov. 2000, doi: 10.1038/35042582.
[14] D. M. Taylor, "Direct cortical control of 3D neuroprosthetic devices," *Science*, vol. 296, no. 5574, pp. 1829–1832, Jun. 2002, doi: 10.1126/science.1070291.
[15] G. Santhanam, S. I. Ryu, B. M. Yu, A. Afshar, and K. V. Shenoy, "A high-performance brain-computer interface," *Nature*, vol. 442, no. 7099, pp. 195–198, Jul. 2006, doi: 10.1038/nature04968.
[16] N. F. Ince, R. Gupta, S. Arica, A. H. Tewfik, J. Ashe, and G. Pellizzer, "High accuracy decoding of movement target direction in non-human primates based on common spatial patterns of local field potentials," *PLoS ONE*, vol. 5, no. 12, Dec. 2010, Art. no. e14384, doi: 10.1371/journal.pone.0014384.
[17] R. D. Flint, E. W. Lindberg, L. R. Jordan, L. E. Miller, and M. W. Slutzky, "Accurate decoding of reaching movements from field potentials in the absence of spikes," *J. Neural Eng.*, vol. 9, no. 4, Aug. 2012, Art. no. 046006, doi: 10.1088/1741-2560/9/4/046006.
[18] T. Pistohl, T. Ball, A. Schulze-Bonhage, A. Aertsen, and C. Mehring, "Prediction of arm movement trajectories from ECoG-recordings in humans," *J. Neuroscience Methods*, vol. 167, no. 1, pp. 105–114, Jan. 2008, doi: 10.1016/j.jneumeth.2007.10.001.
[19] T. Milekovic, "An online brain-machine interface using decoding of movement direction from the human electrocorticogram," *J. Neural Eng.*, vol. 9, no. 4, Aug. 2012, doi: 10.1088/1741-2560/9/4/046003.
[20] D. T. Bundy, M. Pahwa, N. Szrama, and E. C. Leuthardt, "Decoding three-dimensional reaching movements using electrocorticographic signals in humans," *J. Neural Eng.*, vol. 13, no. 2, Apr. 2016, Art. no. 026021, doi: 10.1088/1741-2560/13/2/026021.
[21] O. Talakoub, C. Marquez-Chin, M. R. Popovic, J. Navarro, E. T. Fonoff, C. Hamani, and W. Wong, "Reconstruction of reaching movement trajectories using electrocorticographic signals in humans," *PLoS ONE*, vol. 12, no. 9, Sep. 2017, Art. no. e0182542, doi: 10.1371/journal.pone.0182542.
[22] A. Korik, R. Sosnik, N. Siddique, and D. Coyle, "Decoding imagined 3D arm movement trajectories from EEG to control two virtual arms—A pilot study," *Front Neurosci-Switz*, vol. 12, Mar. 20 2018, doi: 10.3389/fnbot.2019.00094.
[23] Y. J. Kim, "A study on a robot arm driven by three-dimensional trajectories predicted from non-invasive neural signals," *Biomed. Eng. Online*, vol. 14, Aug. 20 2015, doi: 10.1186/s12938-015-0075-8.
[24] R. Sosnik and O. Benzur, "Reconstruction of hand, elbow and shoulder actual and imagined trajectories in 3D space using EEG slow cortical potentials," *J Neural Eng, Nov. 20*, vol. 2019, doi: 10.1088/1741-2552/ab59a7.
[25] A. Korik, R. Sosnik, N. Siddique, and D. Coyle, "Decoding Imagined 3D Arm Movement Trajectories From EEG to Control Two Virtual Arms-A Pilot Study," *Front Neurorobot*, vol. 13, p. 94, 2019, doi: 10.3389/fnbot.2019.00094.
[26] A. Korik, R. Sosnik, N. Siddique, and D. Coyle, "Decoding imagined 3D arm movement trajectories from EEG to control two virtual arms—A pilot study," *Front Neurorobot.*, vol. 13, Nov. 2019, doi: 10.3389/fnbot.2019.00094.
[27] S. Hochreiter and J. Schmidhuber, "Long short-term memory," *Neural Comput*, vol. 9, no. 8, pp. 1735–1780, Nov. 1997.
[28] K. Greff, R. K. Srivastava, J. Koutnik, B. R. Steunebrink, and J. Schmidhuber, "LSTM: A search space odyssey," *IEEE Trans. Neural Netw. Learn. Syst.*, vol. 28, no. 10, pp. 2222–2232, Oct. 2017, doi: 10.1109/tnnls.2016.2582924.
[29] C. Olah. *Web Page*. Accessed: Jan. 27, 2020. [Online]. Available: https://colah.github.io/posts/2015-08-Understanding-LSTMs
[30] J. Fruitet, D. J. Mcfarland, and J. R. Wolpaw, "A comparison of regression techniques for a two-dimensional sensorimotor rhythm-based brain–computer interface," *J. Neural Eng.*, vol. 7, no. 1, Feb. 2010, Art. no. 016003, doi: 10.1088/1741-2560/7/1/016003.

HONG GI YEOM received the B.S. and M.S. degrees in electrical and electronics engineering from Chung-Ang University, in 2008 and 2010, respectively, and the Ph.D. degree in interdisciplinary program in neuroscience from Seoul National University, in 2017. From 2010 to 2011, he was a Research Associate with the Medical Research Center, Seoul National University. Since 2017, he has been an Assistant Professor with the Department of Electronic Engineering, Chosun University. He is the Director of Education, Korean Institute of Intelligent Systems Society (KIIS). His research interests include brain–computer interfaces, brain mechanism, machine learning, and bio signal analysis.

JUNE SIC KIM received the B.S. degree in electrical engineering, and the M.S. and Ph.D. degrees in biomedical engineering from Hanyang University, in 1996, 1998, and 2002, respectively. From 2002 to 2004, he was a Postdoctoral Fellow with McGill University, Montreal, Quebec, Canada. From 2004 to 2014, he was an Assistant Professor with the Seoul National University Hospital. Since 2014, he has been an Associate Professor with the Department of Brain and Cognitive Sciences, Seoul National University. His research interests include brain-computer interfaces, magnetoencephalography, neuroimaging, biomedical image/signal processing, analysis, programming, and computer graphics.

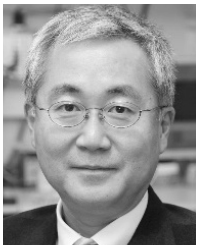

CHUN KEE CHUNG received the M.D. degree from the College of Medicine, Seoul National University, in 1983, and the Ph.D. degree from the Seoul National University, in 1993. From 1983 to 1988, he was an Intern and Resident with the Department of Neurosurgery, Seoul National University Hospital. From 1991 to 1993, he was a Clinical Fellow with the Department of Neurosurgery, Seoul National University Hospital. From 1995 to 1997, he was a Research Fellow with the Department of Neurosurgery, Cleveland Clinic Foundation, OH, USA. From 2006 to 2013, he was a Professor with the Department of Neurosurgery, College of Medicine, Seoul National University. Since 2013, he has been a Professor with the Department of Brain and Cognitive Sciences, Seoul National University. His research interests include brain–machine interfaces, epilepsy, memory, music, sensorimotor interaction, and pain.